sustainability

MDPI

Article

Operating Range, Performance and Emissions of an HCCI Engine Fueled with Fusel Oil/Diethyl Ether: An Experimental Study

Seyfi Polat [1], Alper Calam [2], Seyed Mohammad Safieddin Ardebili [3], Fatih Şahin [4], Alexandru Andrei Boroiu [5] and Hamit Solmaz [4,*]

1 Department of Mechanical Engineering, Faculty of Engineering, Hitit University, Çorum 19030, Turkey
2 Vocational School of Technical Sciences, Gazi University, Ankara 06374, Turkey
3 Department of Biosystems Engineering, Shahid Chamran University of Ahvaz, Ahvaz 61369-84847, Iran
4 Automotive Engineering Department, Faculty of Technology, Gazi University, Ankara 06500, Turkey
5 Department of Automotive and Transport, University of Pitesti, 110040 Pitesti, Romania
* Correspondence: hsolmaz@gazi.edu.tr; Tel.: +90-312-202-8723

Abstract: The main disadvantages of HCCI engines are the knocking tendency at high engine loads, the challenge of the start of the combustion, control of the combustion phase, and the narrow operating range. In this study, we aimed to control the combustion processes in HCCI engines and to expand their working range by improving the fuel properties of fusel oil by the addition of diethyl ether. Thus, the variations in the in-cylinder pressure, rate of heat release, indicated mean effective pressure, start of combustion, combustion duration, CA50, indicated thermal efficiency, mean pressure rise rate, hydrocarbon and carbon monoxide emissions were investigated. It was observed that the in-cylinder pressure and rate of heat release were taken into advance and the test engine could be operated for a wider range by increasing the diethyl ether ratio in the blend. The indicated mean effective pressure increased by 67.5% with DEE40 fuel compared to the DEE80. Under the same operating conditions, HC and CO emissions decreased by 41.6% and 56.2%, in use of DEE40. Furthermore, the highest indicated thermal efficiency was obtained as 42.5% with DEE60 fuel. Maximum hydrocarbon and carbon monoxide emissions were observed with DEE80 fuel as 0.532% and 549 ppm, respectively.

Keywords: fusel oil; diethyl ether; HCCI; combustion; performance; emission

Citation: Polat, S.; Calam, A.; Ardebili, S.M.S.; Şahin, F.; Boroiu, A.A.; Solmaz, H. Operating Range, Performance and Emissions of an HCCI Engine Fueled with Fusel Oil/Diethyl Ether: An Experimental Study. *Sustainability* **2022**, *14*, 15666. https://doi.org/10.3390/su142315666

Academic Editor: Nien-Che Yang

Received: 17 October 2022
Accepted: 17 November 2022
Published: 24 November 2022

1. Introduction

Today, the interest in electric and hybrid vehicles is very high. However, some problems need to be solved, such as drive range, battery technology and how to supply sufficient electrical energy. For this reason, it is predicted that internal combustion engines (ICE) will be used for a while in the near future as the main power source for transportation [1–4].

In many sectors, especially in the transportation sector, fossil fuels are used extensively for energy production. Fossil fuels are gradually decreasing due to the limited resources in the world. The usage of fossil origin fuels with high hydrocarbon content in ICE negatively affects human and environmental health. Increasing the world population and number of vehicles increases greenhouse gas formation and global warming. Governments are continually introducing new legal regulations to reduce exhaust emissions from ICE. In addition, automotive manufacturers are trying to design engines with low specific fuel consumption (SFC) and high thermal efficiency in order to reduce the fuel costs of users. For these reasons, the researchers focused on the use of alternative fuels in ICE, the development of engines with new types of combustion modes with low exhaust emissions and high thermal efficiency [5–15].

Homogeneous charge combustion ignition (HCCI) engines have advantageous features compared to both compression ignition (CI) and spark ignition (SI) engines. In SI engines, the throttling losses occur because the engine power is adjusted by controlling the amount

of air taken into the cylinder using the gas throttle valve. In addition, the high-temperature flame front formed during flame propagation after spark plugs is a source of nitrogen oxide (NOx) emissions. In CI engines, there are problems such as not being able to obtain a homogeneous mixture in the cylinder, knock formation due to long ignition delay time of fuels with a low cetane number, and the inability to provide a simultaneous reduction in soot and NOx emissions. In HCCI combustion mode, the air–fuel mixture is taken into the cylinder almost homogeneously without throttling, and as a result of compression of the mixture, the self-ignition occurs simultaneously at all points of the cylinder. An extremely lean homogeneous mixture is prepared in the cylinder during the intake and compression strokes. Low temperature combustion (LTC) occurs spontaneously in very small crank angles at the end of the compression stroke. Thus, lower NOx and soot emissions can be obtained simultaneously while keeping high thermal efficiency. In addition, the HCCI engine can be run at leaner mixtures than SI engines. However, HCCI engines have some problems and disadvantages that are not fully solved besides the real advantages. While the start of the combustion (SoC) can be controlled easily in SI and CI engines, strict control of the SoC is not possible for HCCI engines. One of the severe problems of HCCI engines is the formation of excessive knocking at high loads and misfire at low loads [16–30].

In order to reduce usage of fossil-based fuels and exhaust emissions, the use of alternative fuels is as important as the use of different combustion modes in ICE. Currently, alcohols are the most important type of fuel that can be used as an alternative to fossil fuels and they can be used in ICE. In addition, alcohols play an important role in reducing emissions since they are oxygen-containing fuels. Ethanol and methanol are among the most common alcohols with their production and production capacities. However, toxic substances in methanol are dangerous for human and environmental health. In addition, ethanol can be easily obtained from sources of vegetable origin such as corn, sugar cane and wheat [31]. Fusel oil is produced as a by-product during the fermentation process of bioethanol and consists largely of amyl alcohol. Recently, 550 k tons of beet molasses were produced annually from 12 million tons of sugar beet in Turkey. Approximately 30 million liters of ethanol were obtained from molasses with these processes. During the distillation of molasses, 1000 liters of ethanol, 1 liter of acetaldehyde, and 5 liters of fusel oil were obtained [32–34].

In recent times, researchers have focused on the use of fusel oil as an alternative fuel in ICE. A detailed overview of the previous studies about the fusel oil usage in ICE, which are SI engines [11,34–55] CI engines [14,33,56–68] and HCCI engines [5,31] can be seen in Figure 1. It seems that there is minimal study for fusel oil usage in HCCI engines while there are many studies for use in SI and CI engines.

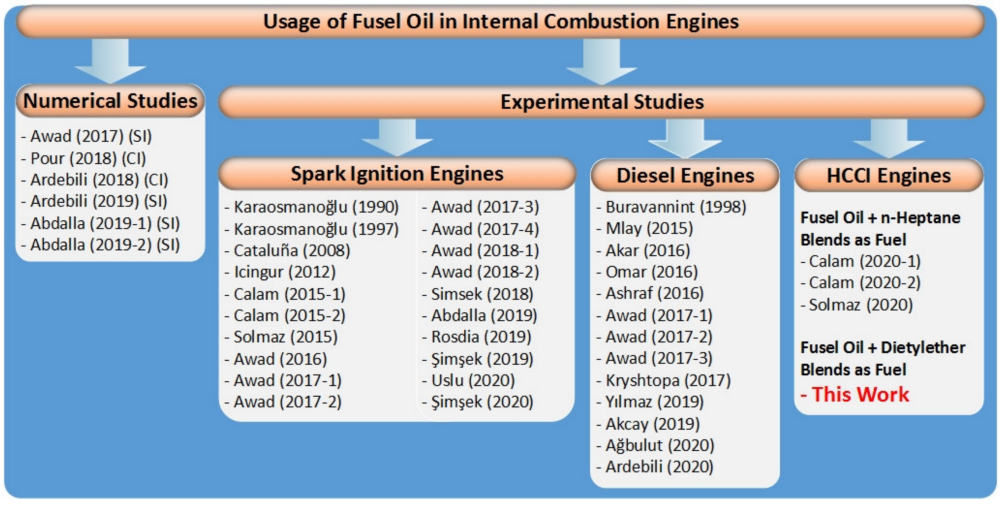

Figure 1. Previous studies about fusel oil usage in ICE. (SI engines [11,34–55] CI engines [14,33,56–68] and HCCI engines [5,31]).

Içingür et al. [47] investigated the effects of the mixtures of fusel oil and gasoline blends on performance and emissions in an SI engine experimentally. It was noted that the highest increase in engine torque was obtained as 3.4% for F30 (30% fusel oil + 70% gasoline as volumetric) blend. It was emphasized that the SFC increased with the increase in the amount of fusel oil in the mixture and the highest increase in the SFC was obtained with F30 as 7.7%. It was also stated that NOx emissions decrease and hydrocarbon (HC) and carbon monoxide (CO) emissions increase as the amount of fusel in the mixture increases. Solmaz [11] examined the effects of fusel oil on performance, combustion and emissions in an SI engine. The study showed that the combustion aggravated and engine performance dropped due to the moisture content and lower heating value (LHV) of the fusel oil. In the study, it was revealed that CO and HC emissions increased up to 25% and 21%, respectively. In addition, NOx emissions decreased about 31% with the usage of fusel oil. Awad et al. [33] investigated the effect of diesel–fusel oil fuel blends on the performance and the emission characteristics in a direct-injected CI engine. It was noted that the brake power and the torque slightly decreased, the indicated SFC increased and the ignition delay duration prolonged with the usage of F20 (80% diesel fuel + 20% fusel oil as volumetric) instead of diesel fuel. It was observed that the NOx emissions decreased and carbon dioxide (CO_2) and CO emissions increased with the usage of fusel oil. It was also emphasized that the reason for the decrease in engine performance was lower cetane index, high moisture content and a lower LHV of fusel oil. Yılmaz [14] investigated the effects of diesel–fusel oil blends on engine performance, combustion and emissions in a direct-injected CI engine. In this study, F5 and F10 fuels were examined in comparison with pure diesel fuel. It was established that the SFC diminished by increasing fusel oil in the blend due to LHV and the water content of fusel oil. It was emphasized that the duration of ignition delay prolonged by increasing the fusel oil rate in the blend owing to a low cetane number of fusel oil. The moisture content of fusel oil reduced NOx emissions by lowering the combustion gas temperatures. However, CO emissions increased since moisture content in fusel oil worsens the combustion process. It was also reported that smoke emissions reduced because of the amount of oxygen content of fusel oil. As a result, it was stated that fusel oil can be used as an alternative fuel additive because it is low-cost fuel and reduces NOx emissions in CI engines. Calam [5] examined the results of the usage of fusel oil in an HCCI engine and presented a detailed report about performance, combustion and emission by using F20, F40 and F60 fuel blends at the intake temperatures of 353 K and 373 K. It was reported that the starting of combustion delayed and the heat release rate occurred more slowly and controlled due the octane increasing effect of fusel oil. It was also emphasized that the indicated thermal efficiency (ITE), HC and CO emissions increased with the increase of fusel oil in the mixture. Sudheesh et al. [69] used diethyl ether as an ignition improver for biogas homogeneous charge compression ignition (HCCI). From their results, it was found that the biogas–DEE HCCI mode shows wider operating load range and higher brake thermal efficiency (BTE) at all loads compared to those of biogas–diesel dual-fuel and biogas SI modes. In addition, they observed that in the HCCI mode, hydrocarbon (HC) emissions are lower than those of the biogas SI mode. Therefore, it is beneficial to use the biogas–DEE HCCI mode while using biogas in internal combustion engines. Polat [10] investigated the effects of diethyl ether–ethanol fuel blends on HCCI combustion, engine performance and exhaust emissions in a single cylinder, port injection HCCI engine experimentally. In the experiments, he used the ethanol and diethyl ether mixtures in different ratios by volume such as 30% ethanol–70% diethyl ether (E30/D70); 40% ethanol–60% diethyl ether (E40/D60); 50% ethanol–50% diethyl ether (E50/D50); and 100% diethyl ether (DEE) as test fuels. He stated that the indicated thermal efficiency increased by about 23.1% and was obtained as 33.1% at $\lambda = 2$ with DEE as compared to E30/D70 at that lambda.

In HCCI engines, the physical and chemical properties of the fuel directly affect the SoC. The most practical way to control the SoC is to increase the intake air temperature (IAT) [30]. However, increasing the IAT too much causes extra energy consumption and decreases the indicated mean effective pressure (IMEP) because of decreasing the volumetric

efficiency [20]. In addition, very high inlet air temperatures increase knock formation in the HCCI engine [30]. Because the octane number of fusel oil makes self-ignition difficult, it limits the operating range of the HCCI engine, especially in poor mixtures. The high octane number of fusel oil causes difficult self-ignition and limits the operation range of HCCI engines, especially with lean mixtures [5]. This disadvantage can be eliminated by mixing fusel oil with other fuels that can easily ignite at lower temperatures so the HCCI engine can be operated in a broader range. The blending of diethyl ether (DEE) and fusel oil can be a useful method for HCCI combustion. DEE has excellent properties such as high oxygen content, latent heat of vaporization, more comprehensive flammability limits, a higher cetane number (>125), reasonable energy density, ignition improvement, cold starting aid and low auto-ignition temperature additive [10,69–72]. This is the first study for the usability of a fusel oil–DEE mixture in HCCI engines. For this reason, it is important to investigate the effects of fusel oil–DEE on combustion, performance and emissions in HCCI engines.

In this study, the effects of DEE–fusel oil blends on performance, combustion and emissions characteristics in an HCCI engine were investigated experimentally. During experiments, three different fuel blends, which are DEE40 (60% fusel oil + 40% diethyl ether as vol.), DEE60 (40% fusel oil + 60% diethyl ether as vol.) and DEE80 (20% fusel oil + 80% diethyl ether as vol.) were used. The experiments were conducted at a constant IAT of 353 K, different engine speed range, and between 1.4 and 4.0 lambda values. The variations in in-cylinder pressure, rate of heat release (ROHR), IMEP, SoC, maximum pressure rise rate (MPRR), combustion duration (CA90-10), combustion phase (CA50), indicated thermal efficiency (ITE), CO and HC emissions were investigated.

2. Materials and Methods

In the present study, a 0.54 L, single-cylinder, four-stroke, port fuel injection Ricardo Hydra brand gasoline engine was operated in HCCI mode. The test engine was operated in spark ignition mode until it reached the operating temperature, then the spark plug ignition was turned off and the experiments were carried out in HCCI mode. The technical specifications of the test engine are shown in Table 1. A schematic view of the experimental testbed is seen in Figure 2. A DC type dynamometer that can absorb 30 kW of power was used in the experiments. The port fuel injection system was used to obtain a homogeneous air/fuel mixture. The potentiometer has high sensitivity on the control panel and was used to adjust the amount of fuel with the pulse width signal of the port fuel injector. 100 equal intervals divided on the potentiometer were used in order to keep the injected fuel rate constant and determine the fuel consumption. Before the experiments, the injector was calibrated by measuring the injection characteristic of the injector for each fuel separately. Thus, the error that may occur in the measurement of fuel mixtures with different viscosity values was eliminated. To calibrate the injector, the amount of each injected fuel blend was measured with a precision balance of 0.01 g for 120 s by adjusting the potentiometer scale on the control panel to 1.0, 2.0, 4.0, 6.0, 8.0 and 10.0 (maximum) at constant engine speed. In this way, the amount of injected fuel, according to the potentiometer position, was determined for each fuel blend. As a result of the calibration of the injector, the quadratic equations of DEE40, DEE60 and DEE80 fuel blends are given in Equations (1), (2) and (3), respectively.

$$y_{DEE40} = [3 \times 10^{-5} \times x^2 + 0.0049 \times x - 0.0019] \times [n/(60 \times 2)] \quad (1)$$

$$y_{DEE60} = [2 \times 10^{-5} \times x^2 + 0.005 \times x - 0.0025] \times [n/(60 \times 2)] \quad (2)$$

$$y_{DEE80} = [1 \times 10^{-5} \times x^2 + 0.0047 \times x - 0.0026] \times [n/(60 \times 2)] \quad (3)$$

Table 1. Engine specifications.

Test Engine	Ricardo Hydra
Number of cylinders	1
Combustion mode	HCCI
Valve lifts Intake-Exhaust [mm]	5.5–3.5
Compression ratio	13
Bore [mm] × Stroke [mm]	80.26 × 88.90
Swept volume [cm^3]	540
Maximum power output (kW)	15
Intake valve O/C timing	12° bTDC 56° aBDC
Exhaust valve O/C timing	56° bBDC 12° aTDC
Port injection pressure (bar)	2.8

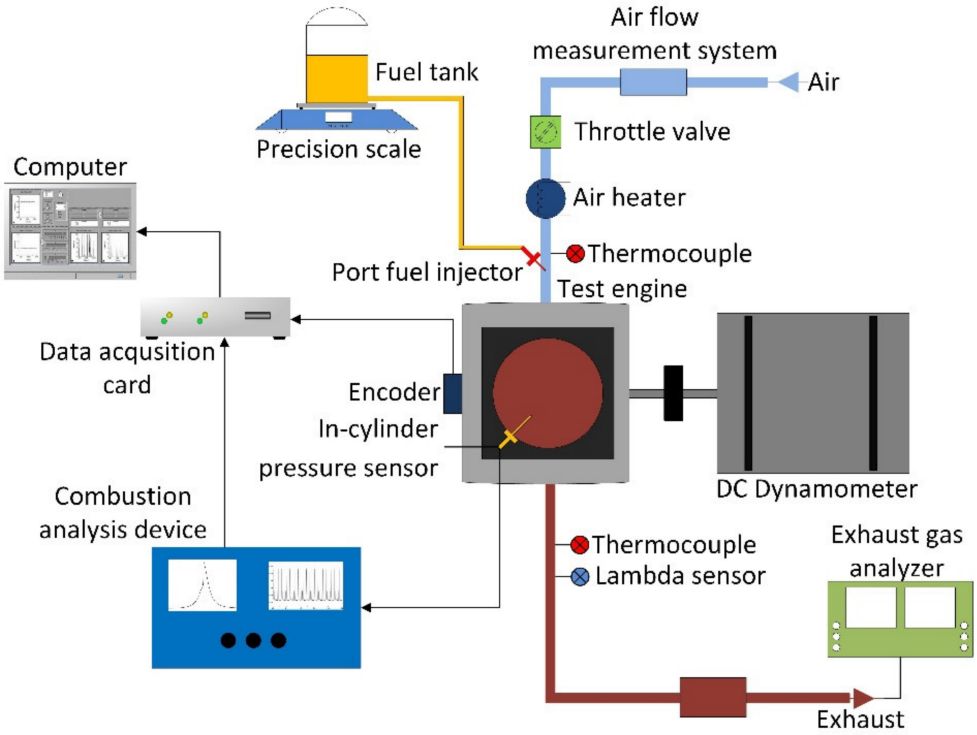

Figure 2. Schematic view of the test bed.

The IAT must be increased in order to achieve HCCI combustion. The air heating system was placed before the intake manifold was used to increase the IAT. The IAT was measured with K type thermocouple located between the air heating system and intake manifold. A closed-loop controller was used to keep the IAT constant. A piezoelectric pressure sensor Kistler 6121 was used to measure the in-cylinder pressure. The technical specifications of pressure sensor are given in Table 2.

Table 2. The technical properties of pressure sensor.

Cylinder Pressure Transducer	Kistler 6121 Piezo Electric
Operating range (bar)	0–250
Measurement precision (pC/bar)	14.7
Operating temperature (°C)	−50 to 350
Accuracy (+/− %)	0.5

Cussons P4110 combustion analyzer was used to increase the received signals from the piezoelectric pressure sensor. The amplified in-cylinder pressure signals were converted to digital signals by using the National Instruments USB 6259 data acquisition card. Moreover, an encoder with a precision of 0.36 CAD was used to determine the crank angle of the test engine. The encoder and amplified in-cylinder pressure signals were recorded to the computer simultaneously to cover at least 50 consecutive cycles. Bosch BEA350 brand exhaust gas analyzer was used for the measure of exhaust emissions. The technical features of the exhaust gas analyzer are presented in Table 3. Additionally, lambda value can measure with an exhaust gas analyzer using the Brettschneider formula.

Table 3. Measurement range and accuracy of the emission analyzer.

	Operating Range	Accuracy
Lambda	0.5–9.999	±0.001
NO (ppm vol)	0–5000	±1
CO (% vol)	0–10	±0.001
O2 (% vol)	0–22	±0.01
HC (ppm vol)	0–9999	±1

The test engine was run in SI mode until the engine coolant temperature reached 65 °C and the engine oil temperature reached 60 °C in order to carry out the experiments under constant conditions. After the test engine had reached the desired temperatures, spark plug ignition was turned off via the control panel, and so HCCI mode was activated. All experiments were carried out under steady-state conditions. Test engine could be run in HCCI mode with DEE40, DEE60 and DEE80 fuels at 800–1400 rpm, 800–1800 rpm and 800–1800 rpm engine speed ranges, 1.4–2.3, 1.4–3.4, 1.8–4.0 lambda ranges, respectively, at constant IAT of 353 K. Ricardo Hydra engine has 9 mm valve lifts for intake and exhaust valves. In order to provide hot exhaust gas recirculation (EGR), we used reduced valve lifts of 5.5 mm for intake valve and 3.5 mm for exhaust valve. Valve lifts were kept constant during all of the experiments.

The amount of fuel injected was controlled via adjusting the position of the potentiometer on the control panel and the data at different lambda values were recorded. The knock limit was determined by the maximum pressure rise rate. The area just before the engine stalls with the impoverishment of the mixture was determined as the misfire limit. In this boundary, coefficient of variance in IMEP was also used to determine the exact misfire border. The region between the knock and misfire boundaries was accepted as the engine's stable operating zone.

Ethyl alcohol is produced by fermenting glucose by yeast. Ethyl alcohol in Turkey, in which the production of sugar from sugar beet molasses is produced from plant-wet beet, pulp is obtained as a byproduct. The sugar rate in molasses content varies according to the sensitivity of sugar production facilities to process sugar beet. In order to recover the sugar in molasses content, it must be fermented under suitable temperature conditions. After the fermentation process, purification and drying, ethyl alcohol is produced with a sensitivity of 99.5%. The wastes under the purification and drying chambers are collected in a tank and this waste product is called fusel oil. Fusel oil is an oil-like mixture waste product with a dark brown to yellow color [47]. Fusel oil consists of 10.2% moisture, 16.16% i-butyl alcohol, 63.03% i-amyl alcohol, 0.686% n-butyl alcohol, 0.688% n-propyl alkyl, 9.236% ethanol. The properties fusel oil, test conditions and some properties of test fuels are shown in Tables 4–6, respectively [10,14,45].

Table 4. Some Properties of Fusel Oil Components Reprinted with permission from Ref. [14]. 2022, Elsevier.

Constituent	Chemical Formula	Molecular Weight (g/mol)	Density (g/cm3)	Boiling Point (°C)	Freezing Point (°C)	Volumetric (%)
i-amyl alcohol	C5H12O	88.148	0.8104	131.1	−117.2	63.03
i-butyl alcohol	C4H10O	74.122	0.802	108	−108	16.16
n-butyl alcohol	C4H10O	74.122	0.8098	117.73	−89.5	0.686
n-propyl alkyl	C3H8O	60.09	0.8034	97.1	−126.5	0.688
Ethanol	C2H6O	46.07	0.789	78.4	−114.3	9.236
Water	H2O	18	1	100	0	10.2

Table 5. Test parameters.

Test Parameters	Value/Description
Engine speed	800–1800 (rpm)
Combustion mode	HCCI
Fuel type	DEE40-DEE60-DEE80
IAT	353 (K)
Lambda range	1.4–4.0
Engine oil temperature	60 °C
Engine water temperature	65 °C

Table 6. Specifications of test fuels.

Fuel	Fusel Oil	Diethyl Ether
Chemical formula	-	C4H10O [10]
Density [kg/m^3]	849 [14]	713.4 [10]
LHV [MJ/kg]	29.5 [14]	33.8 [10]
Research octane number	106.8 [45]	-
Cetane number	42 [14]	>125 [10]
Self-ignition temperature [°C]	416 [14]	160 [10]

A MATLAB code was prepared to calculate the in-cylinder pressure, ROHR, IMEP, CA10, CA90-10, CA50, ITE, and MPRR. The in-cylinder pressure was obtained by averaging 50 consecutive cycles. The ROHR was calculated using the first law of thermodynamics. The gas and mass leaks were neglected in closed-loop cycle analysis. The amount of heat transferred from the cylinder to the cylinder wall was calculated using the modified Woschni model. The variation of the ROHR depending on the crank angle was calculated using Equation (4) [24].

$$\frac{dQ}{d\theta} = \frac{k}{k-1}P\frac{dV}{d\theta} + \frac{1}{k-1}V\frac{dP}{d\theta} + \frac{dQ_{heat}}{d\theta} \quad (4)$$

The polytropic index was calculated using Equation (5) [24].

$$k = -\frac{V \times dP}{P \times dV} \quad (5)$$

The heat transfer to the cylinder wall, which is the last tern in Equation (1), has been calculated according to Newton's cooling law of [24]

$$\frac{dQ_{wall}}{d\theta} = \frac{1}{6n}h_g A\left(T_g - T_w\right) \quad (6)$$

where T_g is in-cylinder gas temperature, T_w is cylinder wall temperature, h_g is heat transfer coefficient and A is instantaneous cylinder wall surface area. In order to calculate heat

transfer coefficient, Woschni's equation, which depends on gas velocity, pressure and temperature in the cylinder, is widely used [27].

$$h_g = \alpha_s L^{-0.2} p^{0.8} T_g^{-0.73} w_{tuned}^{0.8} \quad (7)$$

where L is instantaneous chamber height, w_{tuned} is the characteristic velocity.

The net work and IMEP were calculated using Equations (8) [24] and (9) [24].

$$W_{net} = \int PdV \quad (8)$$

$$IMEP = \frac{W_{net}}{V_{stroke}} \quad (9)$$

The ITE was calculated using Equation (10) [24].

$$\eta_T = \frac{W_{net}}{\dot{m}_{DEE} \times Q_{LHV_{DEE}} + \dot{m}_{fusel\ oil} \times Q_{LHV_{fusel\ oil}}} \quad (10)$$

3. Results

HCCI engines have a limited operating range due to misfire at low loads and knock problems at high loads. The misfiring problem at lean mixtures can be solved by using fuels that have high self-ignition capability and low auto-ignition temperature. Fusel oil, which has the capability to be an alternative to fossil fuels, is difficult to use at low loads in HCCI engines because of the high research octane number. Therefore, the use of fusel oil in combination with a fuel having a high cetane number may allow the HCCI engine to be operated in a wider range.

Figure 3a–c shows that the variation of in-cylinder pressure and ROHR depend on the crank angle with DEE40, DEE60, and DEE80, respectively, at constant engine speed. The ROHR and in-cylinder pressure were taken into advance at low lambda values for all test fuels. The possibility of fuel molecules matching with oxygen molecules increased as the richer mixture was obtained with the increase of lambda value. Thus, the SoC was recorded at an earlier crank angle. Furthermore, the maximum values of the in-cylinder pressure and ROHR increased as the fuel energy driven into the cylinder was increased as a result of the richer mixture. It was also seen that the in-cylinder pressure and ROHR were taken into advance by increasing DEE ratio in the mixture. The auto-ignition ability of the mixture increased as the DEE ratio increased in the mixture since the cetane number of DEE is higher than fusel oil. Therefore, the whole combustion phases were taken in advance. The two combustion stages on ROHR traces, which is a general combustion characteristic of HCCI engines, are seen as in previous studies [73]. In Figure 3a, the higher octane number of DEE40 fuel compared to DEE60 and DEE80 fuels results in a single-stage ROHR. However, the two-stage ROHR was obtained as the DEE ratio increased in the blend because the octane rating decreased and the self-ignition ability increased. As seen in Figure 3c, low-temperature oxidation reactions become more evident using DEE80 fuel. The test engine could be operated with the DEE40 fuel at the range of 1.4–2.3 lambda values, and it could be operated with the DEE80 fuel at the range of 1.8–3.15 lambda values. It was observed that the operating range shifted towards the poor mixture region for higher DEE ratios in the blend.

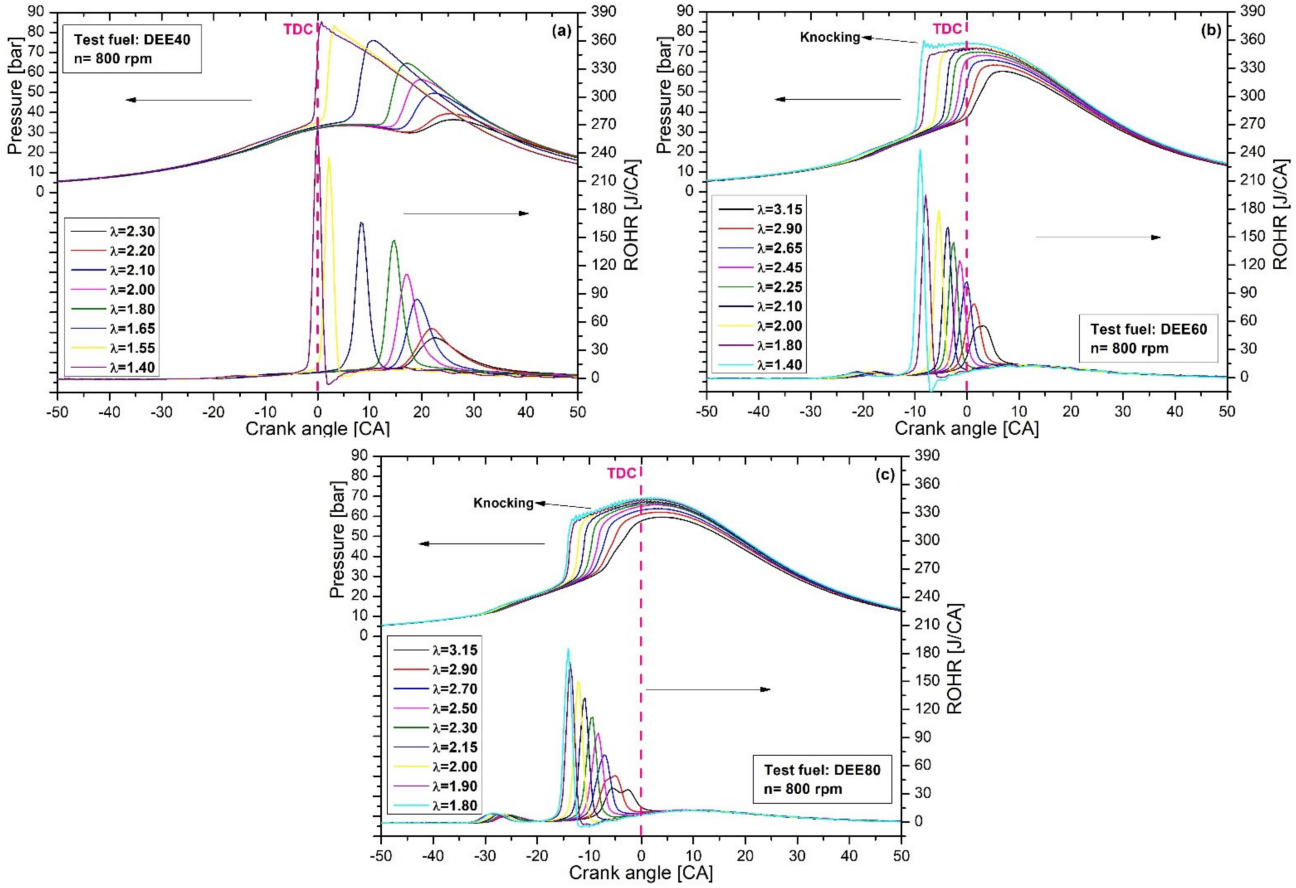

Figure 3. (**a**–**c**) show the variation of in-cylinder pressure and ROHR depend on the crank angle with DEE40, DEE60 and DEE80, respectively, at constant engine speed.

At high loads, the knock formation tended to increase even as the cetane number of the blend was high. For this reason, increasing the DEE ratio in the mixture was limited by knock formation at high loads. At the constant lambda value of 1.8, the peak cylinder pressures were obtained as 65 bar, 72 bar and 69 bar, and the maximum ROHR values were obtained as 147 J/CA, 196 J/CA and 188 J/CA with the DEE40, DEE60 and DEE80 fuels, respectively. A decrease was observed after some increase in the maximum in-cylinder pressure and maximum ROHR with the increase of DEE ratio in the mixture. Firstly, the peak cylinder pressure and maximum ROHR increased by increasing the DEE ratio in the fuel blend, since the LHV of DEE fuel is higher than fusel oil. After that, a decrease occurred in volumetric efficiency in the port fuel injection HCCI engine since the evaporation capacity of DEE fuel was higher than fusel oil. For this reason, the maximum in-cylinder pressure and ROHR decreased again since the fuel energy driven to the cylinder decreased in order to maintain the constant lambda value.

The variation of CA10 with lambda at different fuel blends, which are DEE40, DEE60 and DEE80, is shown in Figure 4. CA10 is defined as the crank angle that represents 10% of the fuel mass burnt fraction and is considered the SoC [31,51,73].

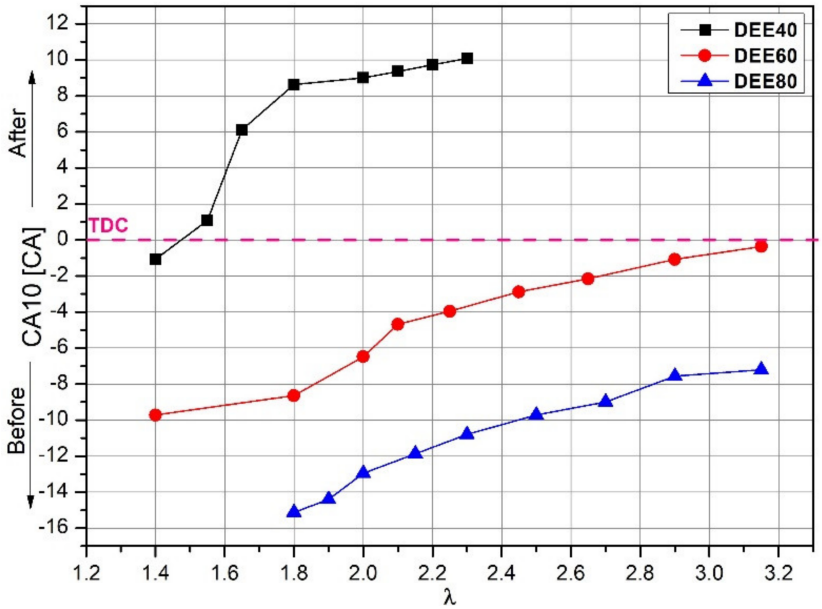

Figure 4. The changing of CA10 with lambda at different fuel blends, which are DEE40, DEE60 and DEE80.

Figure 4 shows the variation of CA10 depending on lambda for different fuel blends, while the start of combustion was delayed in lean mixture conditions for all test fuels as seen in the figure. A poor mixture worsens oxidation reactions and combustion is delayed. This situation causes the combustion duration to be prolonged. With the enrichment of the mixture, the possibility of oxygen and fuel molecules to meet in the cylinder increases. Therefore, chemical reactions start at earlier crank angles than under lean mixture conditions. Rich mixture conditions cause the combustion to be taken in advance. The use of high octane fuel in HCCI engines causes the CA10 to be delayed [17,30]. The increase in the amount of fusel oil in the mixture fuel blend causes an increase in the octane number. This situation causes the CA10 to be delayed. The increase in DEE ratio in the DEE + fusel oil blend increases the cetane number of the blended fuel. Thus, oxidation reactions occur rapidly and combustion starts earlier. It is seen in Figure 4 that the combustion started before the TDC in the use of DEE60 and DEE80 fuels for all lambda values. In the use of DEE40 fuel, it takes place around the TDC and just after the TDC. Figure 4 reveals that the start of combustion can be controlled in HCCI engines by using mixed fuels with different physical and chemical properties.

CA90 is defined as the crank angle that is 90% of the fuel mass burnt in the cylinder and is considered the end of combustion. The period between CA10 and CA90 is expressed as the combustion duration [31,73,74]. The variation of CA10-90 with lambda at different fuel blends, which are DEE40, DEE60 and DEE80, is seen in Figure 5. The combustion duration directly depends on the rate of chemical reactions. The chemical reaction rate is the function of the cylinder gas temperature. Improved chemical kinetic reactions heal combustion, and combustion duration decreases with the increase of the in-cylinder gas temperature.

In Figure 5, the mixture becomes lean and the in-cylinder gas temperature decreases as the fuel energy driven into the cylinder decreases with the increase in the lambda value. The combustion duration prolonged because the low in-cylinder gas temperature caused the chemical kinetic reactions to slow down. As can be seen in Figure 5, the duration of combustion decreased for the fuel blends containing a high DEE ratio. The high cetane number of DEE fuel enables faster combustion reactions. Thus, the duration of combustion shortened by increasing the DEE ratio in the fuel blend. Furthermore, the combustion duration decreased as a result of the combustion process that takes place at a higher temperature since the LHV of the mixture increased for the fuel blends, including a high DEE ratio.

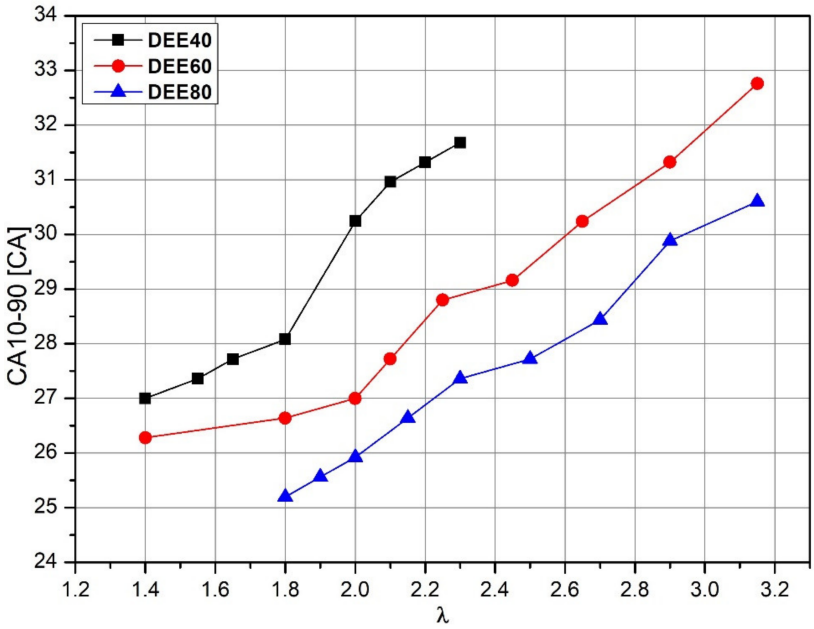

Figure 5. The changing of CA10-90 with lambda at different fuel blends, which are DEE40, DEE60 and DEE80.

Figure 6a,b shows the variation of CA50 and ITE respectively depend on lambda at different fuel blends, which are DEE40, DEE60 and DEE80. CA50 is defined as the location of the 50% of the total fuel energy released in the cylinder in terms of crank angle and is taken into consideration at the midpoint of combustion. In HCCI engines, it is very important to obtain the CA50 slightly after top dead center (TDC) such as 8–10 degrees in terms of engine performance, obtaining the CA50 before TDC increases the negative work on the piston. The obtaining of the CA50 towards the end of the expansion stroke after TDC also adversely affects the net work [17,30,73,75].

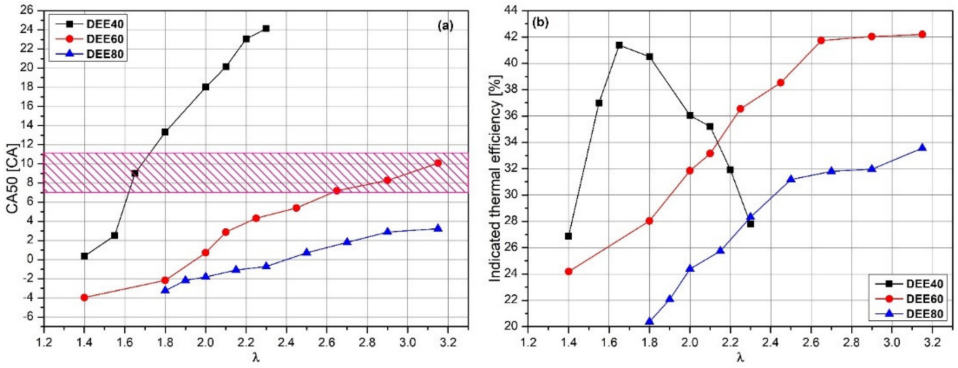

Figure 6. (**a**,**b**) show the variation of CA50 and ITE, respectively, depends on lambda at different fuel blends, which are DEE40, DEE60 and DEE80.

In Figure 6a, it was observed that CA50 was delayed just like CA10 with the increase of lambda value. The in-cylinder gas temperatures increased since the fuel injected into the cylinder was high for rich mixtures. Therefore, the chemical kinetic reactions accelerated, and thus the CA50 was taken into advance. The CA50 is taken into advance with the increase of the DEE ratio in the blend due to the fact that the cetane number and LHV of the mixture increased.

The most important factor affecting thermal efficiency is CA50 [30]. The higher ITE values were obtained at the test points where the CA50 corresponds to the range of 7–11 CA degrees after TDC as shown in Figure 6a,b. In the use of DEE80 fuel, the high reactivity

(high DEE ratio, high cetane number) of the fuel and high LHV causes the combustion to start earlier and the CA50 to occur before the optimum operating conditions. This causes the indicated thermal efficiency to be low in all lambda values. Indicated thermal efficiency in the use of DEE60 fuel is higher than DEE80 for all lambda values. In addition, the highest indicated thermal efficiency was recorded as 42.5% with DEE60 fuel where the lambda was 3.15. DEE60 fuel includes more fusel oil than DEE80 fuel. This increases the octane number of the blended fuel, that is, it decreases the reactivity of the fuel. Thus, combustion was slowed down and HCCI combustion was controlled. In the use of DEE60 fuel, optimum CA50 values were obtained, which ensures maximum indicated thermal efficiency, especially for lambda values below 2.2. In the use of DEE40 fuel, it is seen that the indicated thermal efficiency reaches a peak in a very small operating range, and the thermal efficiency is quite low except for this lambda value. It has been determined that under rich mixture conditions, CA50 occurs immediately after TDC, but with a little lean mixture (lambda = 1.65), the maximum indicated thermal efficiency for this fuel was obtained at the optimum CA50 value. The further impoverishment of the mixture caused the CA50 to be obtained much later than the TDC, depending on the low reactivity of DEE40 fuel and the water content of the fusel oil. This caused the indicated thermal efficiency to decrease sharply due to the expansion of the cylinder volume.

In ICE, MPRR should not exceed 10 bar/CAD because high MPRR conditions cause knocking and unstable working conditions. In addition, knock can seriously damage engine parts [30,73]. Figure 7 shows the variation of MPRR with lambda at different fuel blends, which are DEE40, DEE60 and DEE80. It was seen that the MPRR increased with the decrease of lambda values for all test fuels. This is because of the increased fuel energy driven to the cylinder at low lambda values. The maximum ROHR increased with higher fuel energy. It was observed that the knock limit, which is 10 bar/CAD, was exceeded under rich mixture conditions for all test fuels [30]. When comparing all test fuels at a constant lambda value of 1.8, the highest MPRR value was obtained with DEE80 fuel. The higher pressure was released in a shorter time, as the cetane number of the mixture increased, and the auto-ignition temperature decreased by increasing DEE ratio in the fuel blend. Thus, the MPRR increased.

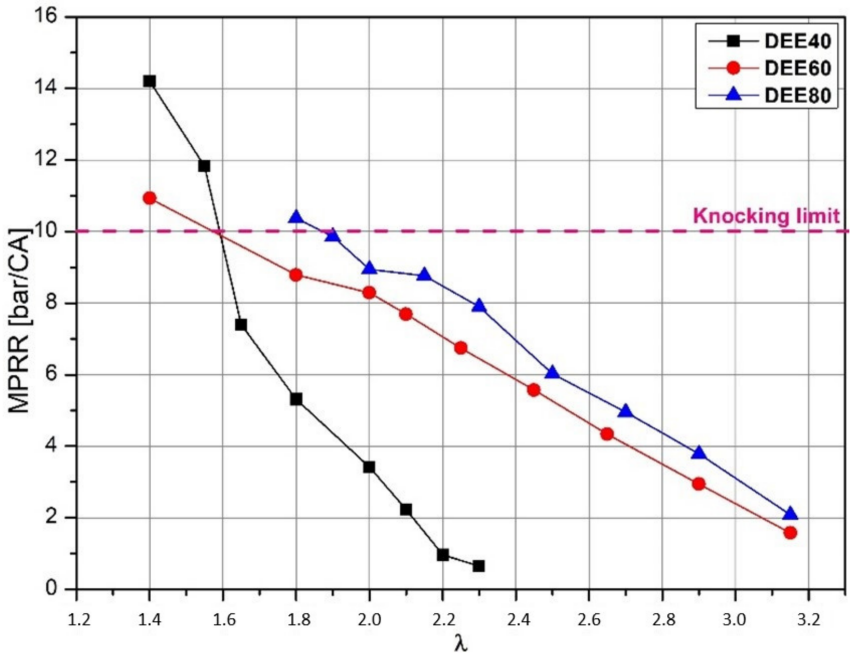

Figure 7. The variation of MPRR with lambda at different fuel blends, which are DEE40, DEE60 and DEE80.

Figure 8 shows the variations of the IMEP at different lambda values, fusel oil/DEE blend ratios and engine speeds. It was seen that IMEP decreased as the lambda value increased for all test fuel blends at given engine speed in Figure 8. The amount of fuel energy driven into the cylinder decreased with the increase in lambda value. Depending on this, the net work and IMEP decreased. The IMEP decreased at high engine speeds for a given constant lambda value for DEE40 fuel. The effective force on the piston decreased with the increase in engine speed since the combustion phase was delayed. The DEE60 and DEE80 fuels were not dominantly affected by the variation of engine speed. It was observed that the operating range shifted towards the poor mixture region, and the test engine could be operated a wider operating range with the increase in the DEE ratio in the blend. The combustion could be obtained without misfire in poorer mixtures by increasing the DEE ratio in the fuel blend since the cetane number increased and the auto-ignition temperature decreased. However, it was observed that IMEP decreased with an increase in the DEE ratio in the fuel blend, as seen in Figure 8. Advancing the CA10, obtaining the CA50 before TDC, shortening the combustion duration and shifting the operating range towards the poor mixture region caused a decrease in IMEP by increasing the DEE ratio in the fuel blend.

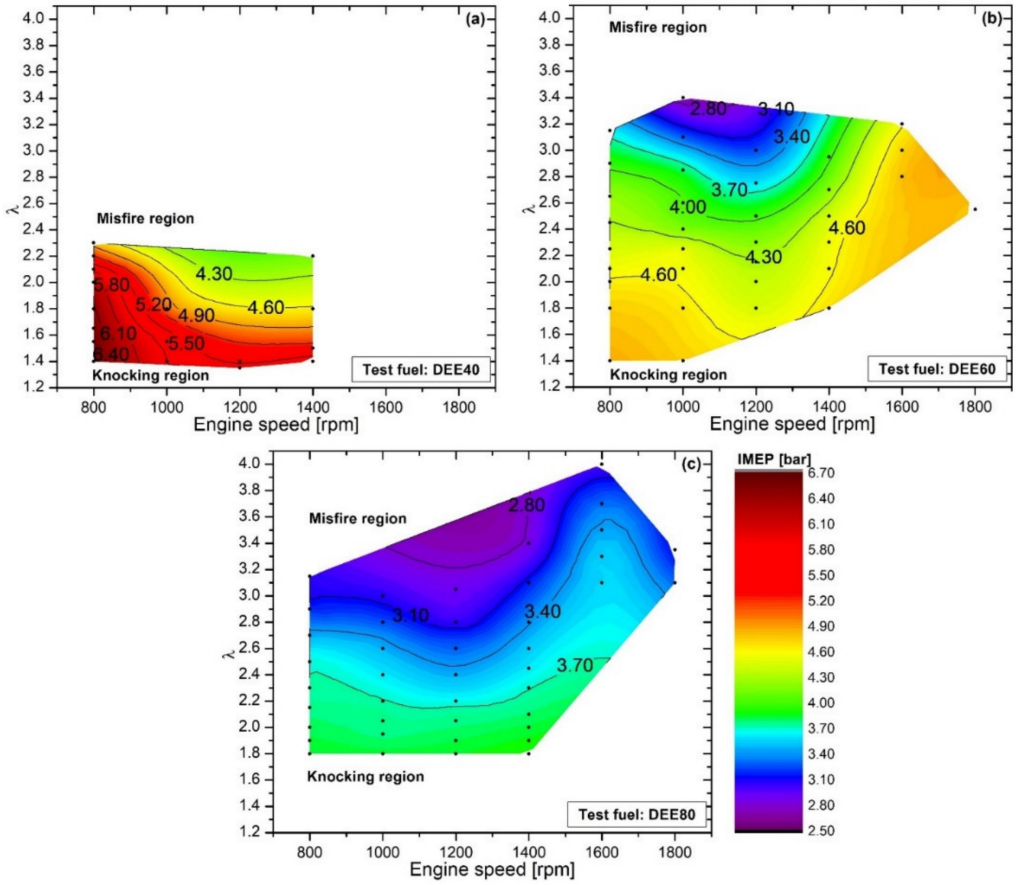

Figure 8. (**a**–**c**) show the variation of IMEP depends on engine speed with DEE40, DEE60 and DEE80, respectively.

HCCI engines can be operated with extremely poor homogeneous mixtures if the suitable working conditions (ideal IAT, supercharging, high compression ratio, EGR rate, etc.) are provided [18,75–77]. As a result of lean combustion, the gas temperatures at the end of combustion reduce, and very low NOx emissions are emitted in HCCI combustion. However, low gas temperatures cause deterioration of oxidation reactions and increase CO and HC emissions [78]. The main reason for the formation of HC emissions is the cavities in the combustion chamber. The air–fuel mixture that settles in the valve and ring grooves

cannot burn. In addition, heat losses occurring in areas close to the cylinder walls cause deterioration of oxidation reactions, and HC emissions increase as well [5,17]. Figure 9a–c shows the variation of HC emission depends on engine speed with DEE40, DEE60 and DEE80, respectively. As the DEE ratio in mixture fuels increased, the HCCI working range expanded, and HC emissions increased under extremely poor mixture working conditions. HC emissions were minimum for all test fuels under rich operating conditions. Because of the increased gas temperatures at the end of combustion at higher loads, HC emissions reduced. The time remaining for combustion decreased with increasing engine speed. Therefore, the increase in engine speed caused an increase in HC emissions for all test fuels. HC emissions increased near the misfire area for all test fuels. The main reason for this was the low combustion gas temperatures. In the operations with extremely lean mixture conditions, cyclic variations increased, the engine ran erratically and HC emissions increased. The highest HC emissions were recorded with the use of DEE80 fuel. DEE improved the poor evaporation properties of fusel oil and was used as a combustion improver in this study. With the increase in the DEE ratio, the octane number of the blend fuels decreased, and the high cetane index of DEE allowed the HCCI working range to expand, but it caused the SoC at earlier crank angles. HCCI combustion, which developed long before the top dead center, caused an increase in negative forces acting on the piston and reduced ITE. This situation caused knocking, especially in rich mixture operation regions. With the increase in MPRR, the combustion pattern deteriorated, and HC emissions increased. The worst HC emissions were recorded with DEE80 fuel at 1600 rpm and 1800 rpm engine speeds. In these conditions, there was not enough time for HCCI combustion, and especially at lean mixture operating conditions, the post-combustion gas temperatures were very low.

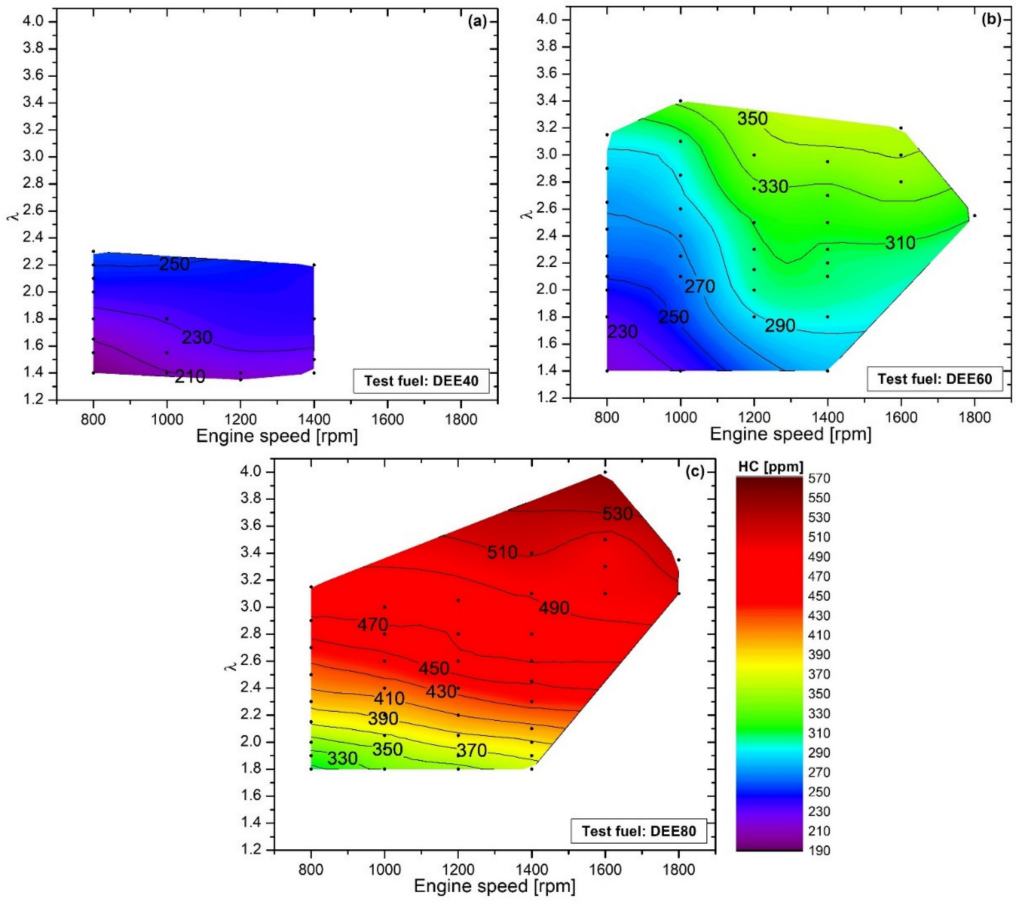

Figure 9. (**a**–**c**) show the variation of HC emission depends on engine speed with DEE40, DEE60 and DEE80, respectively.

CO emissions are sensitively affected by post-combustion gas temperatures. For this reason, CO emissions increase in lean mixture regions of HCCI combustion. With the enrichment of the mixture, oxidation reactions improve, and CO emissions tend to decrease [79,80]. Figure 10a–c shows the variation of CO emission depends on engine speed for DEE40, DEE60 and DEE80 fuels, respectively. With the increase in the DEE ratio in blend fuels, the HCCI operation range expanded. While the high octane number of fusel oil made combustion slower and more controlled, combustion started at earlier crank angles as the ratio of DEE increased in mixture fuels. The fact that the heat release rate took place during the compression time caused deterioration of oxidation reactions and prevented CO from converting to CO2. The lowest CO emissions were achieved with DEE40 fuel, while CO emissions worsened as the DEE ratio increased in mixture fuels. In the use of DEE80 fuel, especially in extremely lean mixture working areas close to the misfire limit, low post-combustion gas temperatures caused CO emissions to increase. However, cyclic variations also increased in the misfire boundary. This is also an indication that oxidation chemistry was impaired. Lack of sufficient time for combustion at high engine speeds (up to 1400 rpm) caused the CO emissions to be increased for all lambda values in the use of DEE80 fuel.

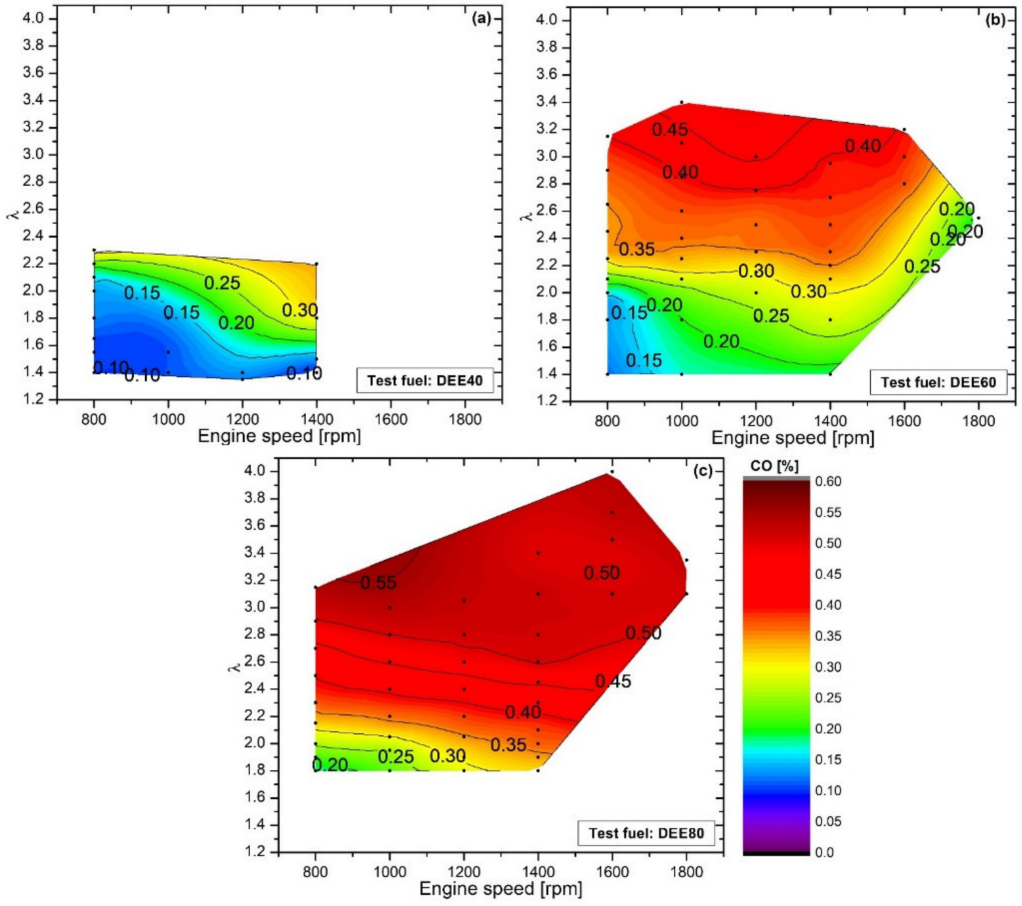

Figure 10. (**a**–**c**) show the variation of CO emission depends on engine speed with DEE40, DEE60 and DEE80, respectively.

4. Discussion

The main challenges of HCCI engines are the knocking at high engine loads, narrow operating range, difficulties about start of the combustion and control of the combustion phase. In this study, we aimed to control the combustion phase in an HCCI engine and to expand the working range by improving the fuel properties of fusel oil, which is a waste product and does not have an economical equivalent, with the addition of diethyl

ether. Thus, in the present study, the effects of fusel oil/DEE fuel blends on performance, combustion and emissions characteristics in a single-cylinder HCCI engine were investigated experimentally. During the experiments, three different fuel blends, which are DEE40, DEE60 and DEE80, were used as the test fuel. The experiments were carried out at constant IAT of 353 K, different engine speeds and between 1.4 and 4.0 lambda values. The variations in in-cylinder pressure, ROHR, IMEP, SoC, CA50, combustion duration, ITE, MPRR, HC and CO emissions were investigated.

It was observed that the in-cylinder pressure and ROHR were taken into advance, the operating range shifted towards the poor mixture region, the SoC and the CA50 advanced, the combustion duration decreased, the MPRR increased, the IMEP decreased, HC and CO emissions increased, and the test engine could be operated a wider operating range with the increase in DEE ratio in the mixture. In addition, the highest ITE was obtained as 42.5% with DEE60 fuel. The addition of DEE to fusel oil improved the fuel properties, and therefore the operating range of the engine expanded. However, the fact that the combustion took place at earlier crank angles caused the oxidation chemistry to deteriorate, increasing the emissions of CO and HC. The highest CO and HC emissions were recorded as 0.532% and 549 ppm in the use of DEE80 fuel at an engine speed of 1600 rpm and lambda of 4.0. High engine speed and extremely lean mixture conditions worsened HC and CO emissions simultaneously.

In summary, the main bullet points of this study are as follows: Fusel oil and DEE fuel blends can be used as an alternative fuel in HCCI engines, the operating range of HCCI engine can be extended by adding DEE into fusel oil, and the auto-ignition ability of the mixture can be increased by adding DEE into fusel oil. DEE can be used in internal combustion engines without major changes in the engine. However, DEE has high volatility and a high flammability. Therefore, it is necessary to increase the precautions in fuel storage systems. However, since fusel oil is an alcohol derivative, it has a high water holding capacity and can cause corrosion. For this reason, the corrosion effects of fusel oil and DEE mixtures should also be investigated. In this study, it can be stated that DEE60 fuel is feasible because HCCI combustion can be controlled and maximum indicated thermal efficiency can be obtained. However, the optimum operating range can be determined by simultaneous control of the compression ratio and EGR in an engine with a variable compression ratio. In addition, it is predicted that HCCI engines can be used in hybrid vehicle technology with alternative fuels due to their high thermal efficiency advantage.

Author Contributions: Conceptualization, S.M.S.A., F.Ş. and H.S.; Methodology, A.C., H.S. and F.Ş.; Formal analysis, S.P.; Investigation, A.C. and H.S.; Data curation, S.P. and S.M.S.A.; Writing–original draft, S.P., A.C., S.M.S.A., F.Ş., A.A.B. and H.S.; Writing–review & editing, S.P., F.Ş., A.A.B. and H.S.; Visualization, A.C. and H.S.; Project administration, H.S. and A.C. All authors have read and agreed to the published version of the manuscript.

Funding: This research received no external funding.

Informed Consent Statement: Not applicable.

Conflicts of Interest: The authors declare no conflict of interest.

References

1. Zeng, X.; Li, M.; Abd El-Hady, D.; Alshitari, W.; Al-Bogami, A.S.; Lu, J.; Amine, K. Commercialization of lithium battery technologies for electric vehicles. *Adv. Energy Mater.* **2019**, *9*, 1900161. [CrossRef]
2. Kocakulak, T.; Solmaz, H. Control of pre and post transmission parallel hybrid vehicles with fuzzy logic method and comparison with other power systems. *J. Fac. Eng. Archit. Gazi Univ.* **2020**, *35*, 2269–2286.
3. Montoya, A.; Guéret, C.; Mendoza, J.E.; Villegas, J.G. The electric vehicle routing problem with nonlinear charging function. *Transp. Res. Part B Methodol.* **2017**, *103*, 87–110. [CrossRef]
4. Liu, J.; Peng, H. Modeling and control of a power-split hybrid vehicle. *IEEE Trans. Control. Syst. Technol.* **2008**, *16*, 1242–1251.
5. Calam, A. Effects of the fusel oil usage in HCCI engine on combustion, performance and emission. *Fuel* **2020**, *262*, 116503. [CrossRef]

6. Calam, T.T. Investigation of the electrochemical behavior of phenol using 1H-1, 2, 4-triazole-3-thiol modified gold electrode and its voltammetric determination. *J. Fac. Eng. Archit. Gazi Univ.* **2020**, *35*, 835–844.
7. Tabanlıgil Calam, T. Analytical application of the poly (1H-1, 2, 4-triazole-3-thiol) modified gold electrode for high-sensitive voltammetric determination of catechol in tap and lake water samples. *Int. J. Environ. Anal. Chem.* **2019**, *99*, 1298–1312. [CrossRef]
8. Calam, T.T. Electrochemical Oxidative Determination and Electrochemical Behavior of 4-Nitrophenol Based on an Au Electrode Modified with Electro-polymerized 3, 5-Diamino-1, 2, 4-triazole Film. *Electroanalysis* **2020**, *32*, 149–158. [CrossRef]
9. Örs, İ.; Sayın, B.; Ciniviz, M. An Experimental Study on the Comparison of the Methanol Addition into Gasoline with the Addition of Ethanol. *Int. J. Automot. Sci. Technol.* **2020**, *4*, 59–69. [CrossRef]
10. Polat, S. An experimental study on combustion, engine performance and exhaust emissions in a HCCI engine fuelled with diethyl ether–ethanol fuel blends. *Fuel Process. Technol.* **2016**, *143*, 140–150. [CrossRef]
11. Solmaz, H. Combustion, performance and emission characteristics of fusel oil in a spark ignition engine. *Fuel Process. Technol.* **2015**, *133*, 20–28. [CrossRef]
12. Uyumaz, A. Combustion, performance and emission characteristics of a DI diesel engine fueled with mustard oil biodiesel fuel blends at different engine loads. *Fuel* **2018**, *212*, 256–267. [CrossRef]
13. Yeşilyurt, M.K.; Doğan, B.; Derviş, E.R.O.L. Experimental assessment of a CI engine operating with 1-pentanol/diesel fuel blends. *Int. J. Automot. Sci. Technol.* **2020**, *4*, 70–89. [CrossRef]
14. Yılmaz, E. Investigation of the effects of diesel-fusel oil fuel blends on combustion, engine performance and exhaust emissions in a single cylinder compression ignition engine. *Fuel* **2019**, *255*, 115741. [CrossRef]
15. Yılmaz, E. A Comparative Study on the Usage of RON68 and Naphtha in an HCCI Engine. *Int. J. Automot. Sci. Technol.* **2020**, *4*, 90–97. [CrossRef]
16. Aydoğan, B. Experimental investigation of tetrahydrofuran combustion in homogeneous charge compression ignition (HCCI) engine: Effects of excess air coefficient, engine speed and inlet air temperature. *Journal of the Energy Institute.* **2020**, *93*, 1163–1176. [CrossRef]
17. Mofijur, M.; Hasan, M.M.; Mahlia, T.M.I.; Rahman, S.A.; Silitonga, A.S.; Ong, H.C. Performance and emission parameters of homogeneous charge compression ignition (HCCI) engine: A review. *Energies* **2019**, *12*, 3557. [CrossRef]
18. Hyvönen, J.; Haraldsson, G.; Johansson, B. Operating conditions using spark assisted HCCI combustion during combustion mode transfer to SI in a multi-cylinder VCR-HCCI engine. In *SAE Technical Paper 2005-01-0109*; SAE: Warrendale, PA, USA, 2005.
19. Cinar, C.; Uyumaz, A.; Solmaz, H.; Topgul, T. Effects of valve lift on the combustion and emissions of a HCCI gasoline engine. *Energy Convers. Manag.* **2015**, *94*, 159–168. [CrossRef]
20. Cinar, C.; Uyumaz, A.; Solmaz, H.; Sahin, F.; Polat, S.; Yilmaz, E. Effects of intake air temperature on combustion, performance and emission characteristics of a HCCI engine fueled with the blends of 20% n-heptane and 80% isooctane fuels. *Fuel Process. Technol.* **2015**, *130*, 275–281. [CrossRef]
21. Rather, M.A.; Wani, M.M. A numerical study on the effects of exhaust gas recirculation temperature on controlling combustion and emissions of a diesel engine running on HCCI combustion mode. *Int. J. Automot. Sci. Technol.* **2018**, *2*, 17–27. [CrossRef]
22. Ferguson, C.R.; Kirkpatrick, A.T. *Internal Combustion Engines: Applied Thermosciences*; John Wiley & Sons: Hoboken, NJ, USA, 2015.
23. Halis, S.; Nacak, Ç.; Solmaz, H.; Yilmaz, E.; Yucesu, H.S. Investigation of the effects of octane number on combustion characteristics and engine performance in a HCCI engine. *J. Therm. Sci. Technol.* **2018**, *38*, 73–84.
24. Heywood, J.B. *Internal Combustion Engine Fundamentals*; McGraw-Hill Education: New York, NY, USA, 2018.
25. Aydoğan, B. Combustion, Performance and Emissions of Ethanol/n-Heptane Blends in HCCI Engine. *Engineering Perspective.* **2021**, *1*, 6–10. [CrossRef]
26. Antunes, J.G.; Mikalsen, R.; Roskilly, A.P. An investigation of hydrogen-fuelled HCCI engine performance and operation. *Int. J. Hydrog. Energy* **2008**, *33*, 5823–5828.
27. Soyhan, H.S.; Yasar, H.; Walmsley, H.; Head, B.; Kalghatgi, G.T.; Sorusbay, C. Evaluation of heat transfer correlations for HCCI engine modeling. *Appl. Therm. Eng.* **2009**, *29*, 541–549. [CrossRef]
28. Starck, L.; Lecointe, B.; Forti, L.; Jeuland, N. Impact of fuel characteristics on HCCI combustion: Performances and emissions. *Fuel* **2010**, *89*, 3069–3077. [CrossRef]
29. Bendu, H.; Murugan, S. Homogeneous charge compression ignition (HCCI) combustion: Mixture preparation and control strategies in diesel engines. *Renew. Sustain. Energy Rev.* **2014**, *38*, 732–746. [CrossRef]
30. Zhao, H. *HCCI and CAI Engines for the Automotive Industry*; Elsevier: Amsterdam, The Netherlands, 2007.
31. Solmaz, H A comparative study on the usage of fusel oil and reference fuels in an HCCI engine at different compression ratios. *Fuel* **2020**, *273*, 117775.
32. Awad, O.I.; Ali, O.M.; Mamat, R.; Abdullah, A.; Najafi, G.; Kamarulzaman, M.; Yusri, I.; Noor, M. Using fusel oil as a blend in gasoline to improve SI engine efficiencies: A comprehensive review. *Renew. Sustain. Energy Rev.* **2017**, *69*, 1232–1242. [CrossRef]
33. Awad, O.I.; Mamat, R.; Ali, O.M.; Yusri, I.M.; Abdullah, A.A.; Yusop, A.F.; Noor, M.M. The effect of adding fusel oil to diesel on the performance and the emissions characteristics in a single cylinder CI engine. *J. Energy Inst.* **2017**, *90*, 382–396. [CrossRef]
34. Calam, A.; Solmaz, H.; Uyumaz, A.; Polat, S.; Yilmaz, E.; İçingür, Y. Investigation of usability of the fusel oil in a single cylinder spark ignition engine. *J. Energy Inst.* **2015**, *88*, 258–265. [CrossRef]
35. Abdalla, A.N.; Ali, O.M.; Awad, O.I.; Tao, H. Wavelet analysis of an SI engine cycle-to-cycle variations fuelled with the blending of gasoline-fusel oil at a various water content. *Energy Convers. Manag.* **2019**, *183*, 746–752. [CrossRef]

36. Abdalla, A.N.; Awad, O.I.; Tao, H.; Ibrahim, T.K.; Mamat, R.; Hammid, A.T. Performance and emissions of gasoline blended with fusel oil that a potential using as an octane enhancer. *Energy Sources Part A Recovery Util. Environ. Eff.* **2019**, *41*, 931–947. [CrossRef]
37. Abdalla, A.N.; Tao, H.; Bagaber, S.A.; Ali, O.M.; Kamil, M.; Ma, X.; Awad, O.I. Prediction of emissions and performance of a gasoline engine running with fusel oil–Gasoline blends using response surface methodology. *Fuel* **2019**, *253*, 1–14. [CrossRef]
38. Awad, O.I.; Mamat, R.B.; Ali, O.M.; Yusri, I.M. Effect of fuel oil-gasoline fusel blends on the performance and emission characteristics of spark ignition engine: A review. *J. Sci. Res. Dev.* **2016**, *3*, 31–36.
39. Awad, O.I.; Mamat, R.; Ibrahim, T.K.; Hagos, F.Y.; Noor, M.M.; Yusri, I.M.; Leman, A.M. Calorific value enhancement of fusel oil by moisture removal and its effect on the performance and combustion of a spark ignition engine. *Energy Convers. Manag.* **2017**, *137*, 86–96. [CrossRef]
40. Awad, O.I.; Mamat, R.; Noor, M.M.; Yusop, F.; Yusri, I.M. The Impacts of Moisture Content on Performance and Emissions of a Four-Cylinder SI Engine Running with Fuse Oil-Gasoline Blends. *WSEAS Trans. Environ. Dev.* **2017**, *13*, 120–128.
41. Awad, O.I.; Mamat, R.; Ibrahim, T.K.; Ali, O.M.; Kadirgama, K.; Leman, A.M. Performance and combustion characteristics of an SI engine fueled with fusel oil-gasoline at different water content. *Appl. Therm. Eng.* **2017**, *123*, 1374–1385. [CrossRef]
42. Awad, O.I.; Mamat, R.; Ali, O.M.; Azmi, W.H.; Kadirgama, K.; Yusri, I.M.; Leman, A.M.; Yusaf, T. Response surface methodology (RSM) based multi-objective optimization of fusel oil-gasoline blends at different water content in SI engine. *Energy Convers. Manag.* **2017**, *150*, 222–241. [CrossRef]
43. Awad, O.I.; Mamat, R.; Ibrahim, T.K.; Kettner, M.; Kadirgama, K.; Leman, A.M.; Saiful, A.I.M. Effects of fusel oil water content reduction on fuel properties, performance and emissions of SI engine fueled with gasoline-fusel oil blends. *Renew. Energy* **2018**, *118*, 858–869. [CrossRef]
44. Awad, O.I.; Ali, O.M.; Hammid, A.T.; Mamat, R. Impact of fusel oil moisture reduction on the fuel properties and combustion characteristics of SI engine fueled with gasoline-fusel oil blends. *Renew. Energy* **2018**, *123*, 79–91. [CrossRef]
45. Calam, A.; İçingür, Y.; Solmaz, H.; Yamık, H. A comparison of engine performance and the emission of fusel oil and gasoline mixtures at different ignition timings. *Int. J. Green Energy* **2015**, *12*, 767–772. [CrossRef]
46. Cataluña, R.; da Silva, R.; de Menezes, E.W.; Ivanov, R.B. Specific consumption of liquid biofuels in gasoline fuelled engines. *Fuel* **2008**, *87*, 3362–3368. [CrossRef]
47. Icingur, Y.; Calam, A. The effects of the blends of fusel oil and gasoline on performance and emissions in a spark ignition engine. *J. Fac. Eng. Archit. Gazi Univ.* **2012**, *27*, 143–149.
48. Karaosmanoglu, F. Evaluation of Alcohol—Gasoline Blends as Engine Fuel Alternative. Ph.D. Thesis, Istanbul Technical University, Istanbul, Turkey, 1990. (In Turkish).
49. Karaosmanoğlu, F.; Işiğigür, A.; Aksoy, H.A. Methanol-unleaded gasoline blends containing fusel oil fraction as spark ignition engine fuel. *Energy Sources* **1997**, *19*, 567–577. [CrossRef]
50. Rosdia, S.M.; Mamata, R.; Azri, A.; Sudhakar, K.; Yusri, I.M. Evaluation of properties on performance and emission to turbocharged SI engine using fusel oil blend with gasoline. *IOP Conf. Ser. Mater. Sci. Eng.* **2019**, *469*, 012113. [CrossRef]
51. Aydoğan, B. Combustion characteristics, performance and emissions of an acetone/n-heptane fuelled Homogenous Charge Compression Ignition (HCCI) engine. *Fuel.* **2020**, *275*, 117840. [CrossRef]
52. Simsek, S.; Ozdalyan, B. Improvements to the composition of fusel oil and analysis of the effects of fusel oil–gasoline blends on a spark-ignited (SI) engine's performance and emissions. *Energies* **2018**, *11*, 625. [CrossRef]
53. Şimşek, S.; Özdalyan, B.; Saygın, H. Improvement of the properties of sugar factory fusel oil waste and investigation of its effect on the performance and emissions of spark ignition engine. *BioResources* **2019**, *14*, 440–452. [CrossRef]
54. Şimşek, S.; Saygın, H.; Özdalyan, B. Improvement of fusel oil features and effect of its use in different compression ratios for an SI engine on performance and emission. *Energies* **2020**, *13*, 1824. [CrossRef]
55. Uslu, S.; Celik, M.B. Combustion and emission characteristics of isoamyl alcohol-gasoline blends in spark ignition engine. *Fuel* **2020**, *262*, 116496. [CrossRef]
56. Ağbulut, Ü.; Sarıdemir, S.; Karagöz, M. Experimental investigation of fusel oil (isoamyl alcohol) and diesel blends in a CI engine. *Fuel* **2020**, *267*, 117042. [CrossRef]
57. Akar, M.A.; Yilmaz, A.; Bas, O.; Keskin, A. Performance and exhaust emissions of diesel engine fueled with Fusel Oil. *J. Biotechnol.* **2016**, *231*, S48. [CrossRef]
58. Akcay, M.; Ozer, S. Experimental investigation on performance and emission characteristics of a CI diesel engine fueled with fusel oil/diesel fuel blends. *Energy Sources Part A Recovery Util. Environ. Eff.* **2019**, *2019*, 1–16. [CrossRef]
59. Awad, O.I.; Mamat, R.; Ali, O.M.; Othman, M.F.; Abdullah, A.A. Experimental study of performance and emissions of fusel oil-diesel blend in a single cylinder diesel engine. *Int. J. Eng. Technol.* **2017**, *9*, 138. [CrossRef]
60. Awad, O.I.; Mamat, R.; Noor, M.M.; Ibrahim, T.K.; Yusri, I.M. Performance, combustion characteristics and emission tests of single cylinder engine running on fusel oil-diesel blended (F20) fuel. *Int. J. Veh. Struct. Syst.* **2017**, *9*, 195–198.
61. Buravannint, S. *Effect of Fusel Oil on Polycyclic Aromatic Hydrocarbons from Exhaust Emission of Diesel Engine*; Chulalongkorn University: Bangkok, Thailand, 1998.
62. Pour, A.H.; Ardebili, S.M.S.; Sheikhdavoodi, M.J. Multi-objective optimization of diesel engine performance and emissions fueled with diesel-biodiesel-fusel oil blends using response surface method. *Environ. Sci. Pollut. Res.* **2018**, *25*, 35429–35439. [CrossRef]

63. Minja, R.J.; Mlay, H.; Katima, J.H. Plant Oil/Fusel Oil Blends as Alternative Fuels in Low-and Medium Speed Diesel Engines. *Am. J. Energy Sci.* **2015**, *2*, 9–16.
64. Ashraf, M. *Summarizing on the Effect of Adding Fusel Oil to Diesel on the Performance and the Emissions Characteristics in a Single Cylinder CI Engine*; Mechanical System Design, Universiti Malaysia Pahang: Pekan, Malaysia, 2016.
65. Mhassan, O. *Mechanical System Design Performance and Emission Parameters of Single Cylinder Diesel Engine Using Fusel Oil-Diesel Blend*; Mechanical System Design, Universiti Malaysia Pahang: Pekan, Malaysia, 2016.
66. Ardebili, S.M.S.; Taghipoor, A.; Solmaz, H.; Mostafaei, M. The effect of nano-biochar on the performance and emissions of a diesel engine fueled with fusel oil-diesel fuel. *Fuel* **2020**, *268*, 117356.
67. Safieddin Ardebili, S.M.; Zaki Dizaji, H.; Sheikh Davoodi, M.J. Optimization of performance and Emission Characteristic of Fusel Oil–Diesel blends Using Response Surface Methodology. *Fuel Combust.* **2018**, *10*, 93–104.
68. Kryshtopa, S.; Kryshtopa, L.; Melnyk, V.; Dolishnii, B.; Prunko, I.; Demianchuk, Y. Experimental research on diesel engine working on a mixture of diesel fuel and fusel oils. *Transp. Probl.* **2017**, *12*, 53–63. [CrossRef]
69. Sudheesh, K.; Mallikarjuna, J.M. Diethyl ether as an ignition improver for biogas homogeneous charge compression ignition (HCCI) operation-An experimental investigation. *Energy* **2010**, *35*, 3614–3622. [CrossRef]
70. Paul, A.; Bose, P.K.; Panua, R.; Debroy, D. Study of performance and emission characteristics of a single cylinder CI engine using diethyl ether and ethanol blends. *J. Energy Inst.* **2015**, *88*, 1–10. [CrossRef]
71. Rakopoulos, D.C.; Rakopoulos, C.D.; Giakoumis, E.G.; Dimaratos, A.M. Characteristics of performance and emissions in high-speed direct injection diesel engine fueled with diethyl ether/diesel fuel blends. *Energy* **2012**, *43*, 214–224. [CrossRef]
72. Cinar, C.; Can, Ö.; Sahin, F.; Yucesu, H.S. Effects of premixed diethyl ether (DEE) on combustion and exhaust emissions in a HCCI-DI diesel engine. *Appl. Therm. Eng.* **2010**, *30*, 360–365. [CrossRef]
73. Polat, S. An experimental investigation on combustion, performance and ringing operation characteristics of a low compression ratio early direct injection HCCI engine with ethanol fuel blends. *Fuel* **2020**, *277*, 118092. [CrossRef]
74. Kodavasal, J.; Lavoie, G.A.; Assanis, D.N.; Martz, J.B. The effects of thermal and compositional stratification on the ignition and duration of homogeneous charge compression ignition combustion. *Combust. Flame* **2015**, *162*, 451–461. [CrossRef]
75. Uyumaz, A. An experimental investigation into combustion and performance characteristics of an HCCI gasoline engine fueled with n-heptane, isopropanol and n-butanol fuel blends at different inlet air temperatures. *Energy Convers. Manag.* **2015**, *98*, 199–207. [CrossRef]
76. Johansson, T.; Johansson, B.; Tunestål, P.; Aulin, H. *HCCI Operating Range in a Turbo-Charged Multi Cylinder Engine with VVT and Spray-Guided DI*; SAE World Congress: Warrendale, PA, USA, 2009; pp. 1–13.
77. Zheng, M.; Han, X.; Asad, U.; Wang, J. Investigation of butanol-fuelled HCCI combustion on a high efficiency diesel engine. *Energy Convers. Manag.* **2015**, *98*, 215–224. [CrossRef]
78. Aydoğan, B. An experimental examination of the effects of n-hexane and n-heptane fuel blends on combustion, performance and emissions characteristics in a HCCI engine. *Energy* **2020**, *192*, 116600. [CrossRef]
79. Aceves, S.M.; Flowers, D.L.; Westbrook, C.K.; Smith, J.R.; Pitz, W.; Dibble, R.; Christensen, M.; Johansson, B. A multi-zone model for prediction of HCCI combustion and emissions. *SAE Trans.* **2000**, *109*, 431–441.
80. Epping, K.; Aceves, S.; Bechtold, R.; Dec, J.E. *The Potential of HCCI Combustion for High Efficiency and Low Emissions*; SAE Technical Paper No. 2002-01-1923; SAE: Warrendale, PA, USA, 2002.